FREQUENCY ANALYSIS OF SURFACE PRESSURES ON AN AIRFOIL AFTER STALL

K.E. Swalwell, J. Sheridan and W.H. Melbourne
Department of Mechanical Engineering
Monash University, Victoria, Australia

ABSTRACT

At high angles of attack airfoils can be considered as bluff bodies and their shedding frequency can be important to designers if it becomes too close to the natural frequency or a harmonic of the natural frequency of the object. This paper details the results from a thick, symmetric airfoil, a NACA 0021 section, at a Reynolds number of 2.70×10^5. At high angles of attack shedding frequencies were found in both the lift and the drag. The main frequency was at half the frequency of the secondary frequency as would be expected for a bluff body although the asymmetry in the wake caused both frequencies to be present in the lift and drag. These frequencies could be scaled by the width of the chord normal to the freestream such that the Strouhal number was nearly constant with angle of attack. The major shedding peak occurred at an angle of attack of 50 degrees, predominately in the lift.

NOMENCLATURE

c	Airfoil chord length (m)
c_d	Sectional coefficient of drag ($=D/½\rho cV^2$)
c_l	Sectional coefficient of lift ($=L/½\rho cV^2$)
D	Drag force (N)
f	Shedding frequency (Hz)
I_u	Stream wise turbulence intensity (%)
l	Length scale (m)
L	Lift force (N)
St	Strouhal number ($St = fl/V$)
V	Tunnel flow velocity (m/s)
α	Angle of attack (degrees)
ρ	Density (kg/m^3)

INTRODUCTION

The aerodynamics of Horizontal Axis Wind Turbines (HAWTs) are complicated, models must account for the variable direction and speed of the natural wind and the rotation of the blades. In addition many HAWTs are designed for the blades to stall in high winds, thereby limiting the forces on the rotor. The thick sections used at the root of wind turbine blades are the first to stall. Difficulties in predicting the aerodynamic performance of wind turbines around stall[1] prompted this investigation into the behavior of thick airfoil sections during and post stall. For simplicity a thick, symmetric airfoil, the NACA0021, was chosen. As part of this investigation the pressure signals obtained from the surface of this airfoil were analyzed for their frequency content.

Post stall airfoils are bluff bodies. Shedding of vortices from bluff bodies causes fluctuating forces on the bodies. Designers must ensure that the shedding frequency does not coincide with the natural frequency of the body or a harmonic of this frequency. Some large wind turbines have suffered from stall-induced vibrations. This has prompted increased interest in the structural response of wind turbines to stall induced vibrations, for example the recent paper by Hansen[2]. The shedding from a thick, symmetric airfoil could also be of interest to designers of other structures who are required to use such airfoils at high α.

For a stationary circular cylinder vortices are alternately shed from the top and bottom surfaces of the cylinder and braid together to form a Kármán street. The vortices shed from the top surface are of negative sign and pull the cylinder up and in the direction of the flow; the vortices shed from the bottom of the cylinder are of positive sign and pull the cylinder down but still in the direction of the flow. The vortex shed from the top of the cylinder results in a peak in the lift force and in the drag. The vortex shed from the bottom of the cylinder results in a trough in the lift force but another peak in the drag. This results in the drag force oscillating at twice the frequency of the lift.

Stalled airfoils have long been known to produce vortex wakes, as discussed for instance in the work of Fage & Johansen in 1928[3]. This compared measurements in the wake of several bluff bodies including two asymmetric bodies, an inclined flat plate and an airfoil section at various α. They measured the boundaries of the vortex sheets at several positions in the near wake. The vortex sheets were found to shed from the leading and trailing edges of the airfoil but did not join in the near wake, although the vortex sheets did expand and therefore became closer to each other. The distance between the sheets increased with α and therefore the vertical distance between the leading and trailing edges increased. Fage & Johansen's[3] most important conclusion was that the frequency and spacing

of vorticity in the wake was dependent on the lateral spacing between the vortex sheets.

Their second conclusion was in part the impetus for Roshko's definition[4] of a universal Strouhal number based on a length scale equal to the width of the wake. Chen & Fang in 1996[5] studied flat plates with beveled sharp edges and found that the *St* based on the width of the plate normal to the freestream remained approximately constant over a range of $0<\alpha<90$ degrees, a small variation being most evident for $\alpha<45$ degrees. They found jumps in *St* associated with the changing of shedding position from the back to the front edge of the bevel.

This paper looks at shedding from a NACA 0021 airfoil, at a reasonably high *Re* of 2.70×10^5 to discover features which may be of interest to designers of machinery such as stall controlled HAWTs which are required to operate at high angles of attack.

EXPERIMENTAL METHOD

The experiments were conducted in the 2m × 1m working section of Monash University's 450kW wind tunnel. The flow over the model was improved by the use of endplates. The NACA 0021 section had circular endplates attached to it, which slotted into circular gaps in the main endplates and allowed the α of the model to be changed while the tunnel was running so hysteresis could be detected.

The model spanned the 1m horizontal section of the tunnel and the chord length of 125mm was chosen so the aspect ratio was greater than seven. This follows the recommendations of Szepessy & Bearman[6] who tested another bluff body, a circular cylinder, at various aspect ratios and found that small aspect ratios could substantially increase the fluctuating lift force, the effect being dependent on *Re*; Szepessy & Bearman tested a *Re* range of 1×10^5 to 1.6×10^6. In the lower end of the range ($Re < 2\times10^5$) decreasing aspect ratio could decrease the fluctuating lift force, whereas at the upper end ($Re = 1.3\times10^5$) the smaller aspect ratios could suppress vortex shedding. This aspect ratio also ensured that the maximum blockage was small (6.25%). No blockage correction was applied to the results.

The model itself was constructed of two carbon fiber shells which were supported by wooden formers which had two steel bars running through them for added strength and stiffness. One of these steel bars was at ¼*c* and was used as the rotation point. The carbon fiber shells had 68 metal pressure taps of internal diameter 1 mm inserted into them level with the surface. These were arranged in 5 rows as shown in Figure 1(a). The rows designated A only had four taps each in them, which are shown by circles in Figure 1(b). The results in this paper came from the complete tapping rows designated Row B1 and B2 in Figure 1(a) and containing all of the taps shown in Figure 1(b). In the rows designated B taps were numbered from the trailing edge (tap 1) across the top surface to the leading edge (tap 15) and then along the bottom surface (to tap 28). The taps were concentrated towards the leading edge in these rows to better determine the high pressure gradients expected in this area. The model was aligned to $\alpha=0$ by equalizing the pressure on the top and bottom surface of the model.

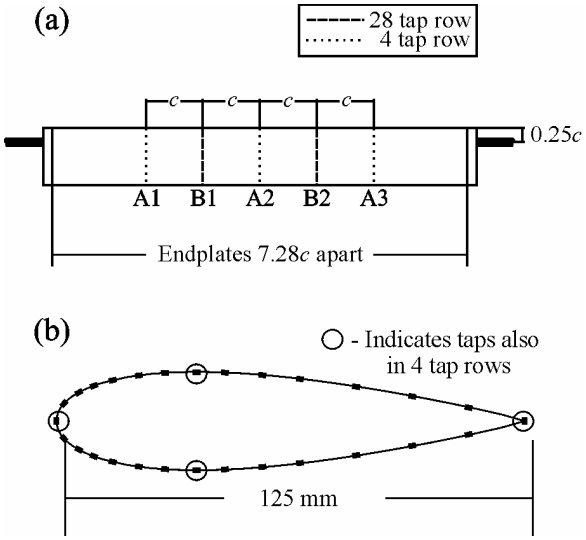

Figure 1 - Tapping placements along airfoil section (a) and around airfoil section (b).

The metal taps were connected by 1.7 m plastic tubing of ID 1mm to an electronic Scanivalve. At each α each tap was sampled at 1000 Hz for 35 seconds. The taps were not all sampled simultaneously however the lag between any two samples was very small, being less than 0.8 ms, and so was unlikely to affect the results. During the runs the dynamic pressure was determined by a Pitot upstream and above the model. This allowed the coefficient of pressure for each sample to be determined.

The flow between the endplates was characterized by Cobra probe traverses. It was found to have a turbulence intensity of $I_u = 0.6\%$ and variations in *V* of less than 3% over the central 0.3m × 0.3m area. The flow decelerated over the distance from the Pitot to the section containing the model but this caused an error in velocity of less than 6% and was not corrected for. The *Re* of the experiment based on the Pitot measurements was 2.70×10^5.

The measurements were corrected for the amplitude and phase response of the tubing by the method detailed by Irwin, Cooper & Girard[7]. The response of the 1.7m tubing was measured experimentally by feeding a pressure signal of known frequency and determining the change in phase and amplitude at the end of the tubing. As can be seen from the Figure 2(a) the tubing reduces the amplitude of signals above 200 Hz by around half or more. The method corrects for this but also amplifies any noise in this region. As there are expected to be no frequencies of interest in this region and any noise will have been substantially amplified all signals above 200 Hz were ignored. As the correction method used fast Fourier transforms this method gave 2^{15} samples.

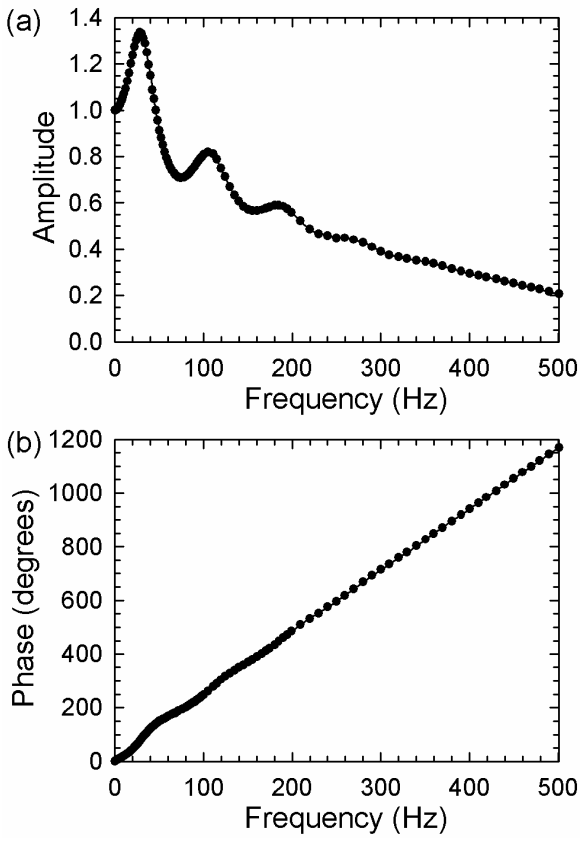

Figure 2 - Tubing response amplitude (a) and phase (b).

The corrected pressure measurements were fitted with a spline function across the surface. The lift and drag were computed from the pressures on these small surfaces for each time step. This gave a lift and drag signal which could be analyzed for frequency content. The frequency content of the signals was analyzed using Matlab's implementation of the Welch method over small segments. The signals were broken into eight segments with 50% overlap. Each of these segments was windowed with a Hamming window. The Power Spectral Density of these segments was then determined and the final result averaged to give a clearer indication of the frequency content of the signals. These results are presented after a brief examination of the mean lift and drag curves.

RESULTS AND DISCUSSION

At low α the lift curve shown in Figure 3(a) shows a linear attached flow region. For $10<\alpha<17.5$ degrees there is a hysteresis loop in the lift curve during stall which also appears in the drag curve, shown in Figure 3(b), due to the jump in drag associated with stall. The lift force calculated using the pressure tap measurements from Rows B1 and B2 are different during the hysteresis loop due to the highly three dimensional nature of this flow. However, while this region is interesting, the current paper is concerned with frequencies experienced post stall, which for the purpose of this paper will be considered as $\alpha > 20$ degrees.

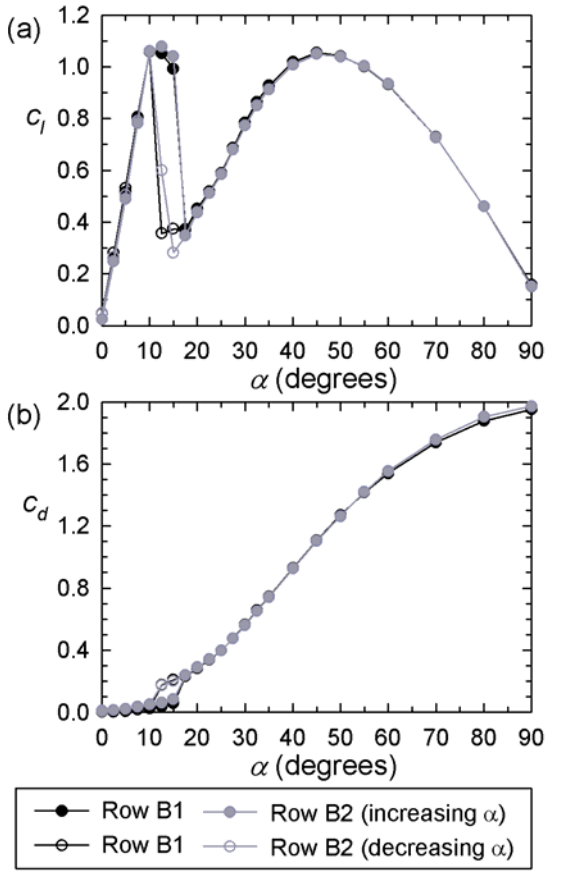

Figure 3 - Forces on aerofoil section versus angle of attack (α), (a) coefficient of lift (c_l) and (b) coefficient of drag (c_d). Open circles indicate that the angle of attack was decreased while the tunnel was running; closed circles indicate the angle of attack was increased.

After stall the lift force increases to a peak at α = 45°. This behavior is similar to a flat plate at 45° where the lift is due to deflection of flow by the bottom surface. As α is increased further the lift force decreases. Interestingly at α = 90° there is still a finite lift force. This is probably due to the flow being able to remain attached for longer around the curved leading edge of the airfoil and separating abruptly at the sharp trailing edge thereby producing a wake which is slightly deflected downwards. The drag curve increases as α increases, as would be expected.

As discussed above, after the pressure measurements were corrected for the response of the tubing, c_l and c_d were calculated for each sample and the Power Spectral Density (PSD) of these lift and drag signals was calculated. These are shown for representative α in Figure 4. For all cases the curves for Row B1 and B2 are very similar. In the lift signal at α = 30° there is a small peak around 100 Hz with some evidence of a peak of similar magnitude at very low frequencies. Peaks at similar frequencies but with much smaller magnitude can just be seen in the drag signal. With a symmetric bluff body, such as a cylinder, the frequency in the drag would be expected to be at twice the frequency in the lift as explained in the Introduction. However as this body is asymmetric it has a mean lift and drag. It seems reasonable that the vortices would follow the wake downwards and therefore affect both the lift and drag. Furthermore, because of the separation of the two vortex sheets, taps closer to one sheet are likely to be influenced much more by that sheet than the other thereby giving the same frequency to the lift and drag. At α = 30° the mean lift force is much higher than the mean drag force (see Figure 3) which may explain the difference in magnitude of the fluctuations.

At α = 50° there is a very strong peak at around 60 Hz in both the lift and drag signals, although the peak is about twice as strong in the lift. Interestingly, at this α the mean lift and the drag forces are similar in magnitude. There are also low frequency signals in both the lift and drag. Secondary peaks are evident in both the lift and drag at 125 Hz but are of very low magnitude and barely visible at the scale of Figure 4. This secondary peak could be from the vortices shed from the leading and trailing edge both influencing some taps. It is possible this secondary peak is showing up in the lift due to slight bleeding of the drag force into the lift force due to slight inaccuracies in α, evident in the slightly positive lift at α=0° in Figure 3. However the explanation of the deflection of the wake is considered more likely.

When the α = 70° is compared to the α = 50° case the strong peak can be seen to have reduced in magnitude in both lift and drag and the frequency has decreased to 50 Hz. There are some low frequencies present in the lift but they too are of smaller magnitude than in the α = 50° case. The secondary peak is barely visible in the lift signal. However the low frequency peak in the drag signal has strengthened and there is also a small peak at about 100 Hz.

At α = 90° the strong peak in the lift case has reduced in magnitude and slightly in frequency, down to about 45 Hz. There are no low frequencies or secondary peaks visible. However in the drag signal the low frequencies provide the highest magnitude components and the main shedding peak is not visible but the secondary peak at about 90 Hz is larger than in the 70° case.

Figure 5(a) shows the frequency of the shedding peaks at various α. Both the main shedding peak and the secondary one, expected to be at twice the frequency of the main peak, are plotted. The decline in shedding frequency with α is similar to that observed by Chen & Fang[5] for a flat plate at various α, as described in the Introduction. Similarly, this shedding frequency and the chord length normal to the freestream velocity were used to determine *St*, which is plotted in Figure 5(b). It can be seen that this is nearly constant value for both the first and second frequencies, which is reasonable given that the wake width would be expected to increase with increasing α.

Earlier it was suggested as the angled wake is angled downwards the main and secondary shedding frequencies could be evident in both the lift and the drag. The secondary frequency is weak, probably because the two vortices shed from the leading edge and trailing edge are a fair distance apart and do not interact much near the body. The difference in relative magnitude of the two peaks can clearly be seen in the difference of scale needed to look at their magnitude (see Figure 5(c) and (d)).

The secondary peak in the drag increases to α = 90° but peaks in the lift at $\alpha \approx$ 50° as would be expected from the above hypothesis. The strongest shedding is observed in the first shedding peak at $\alpha \approx$ 50°. Why this is so deserves further investigation, to do so the frequencies seen by each tap were determined.

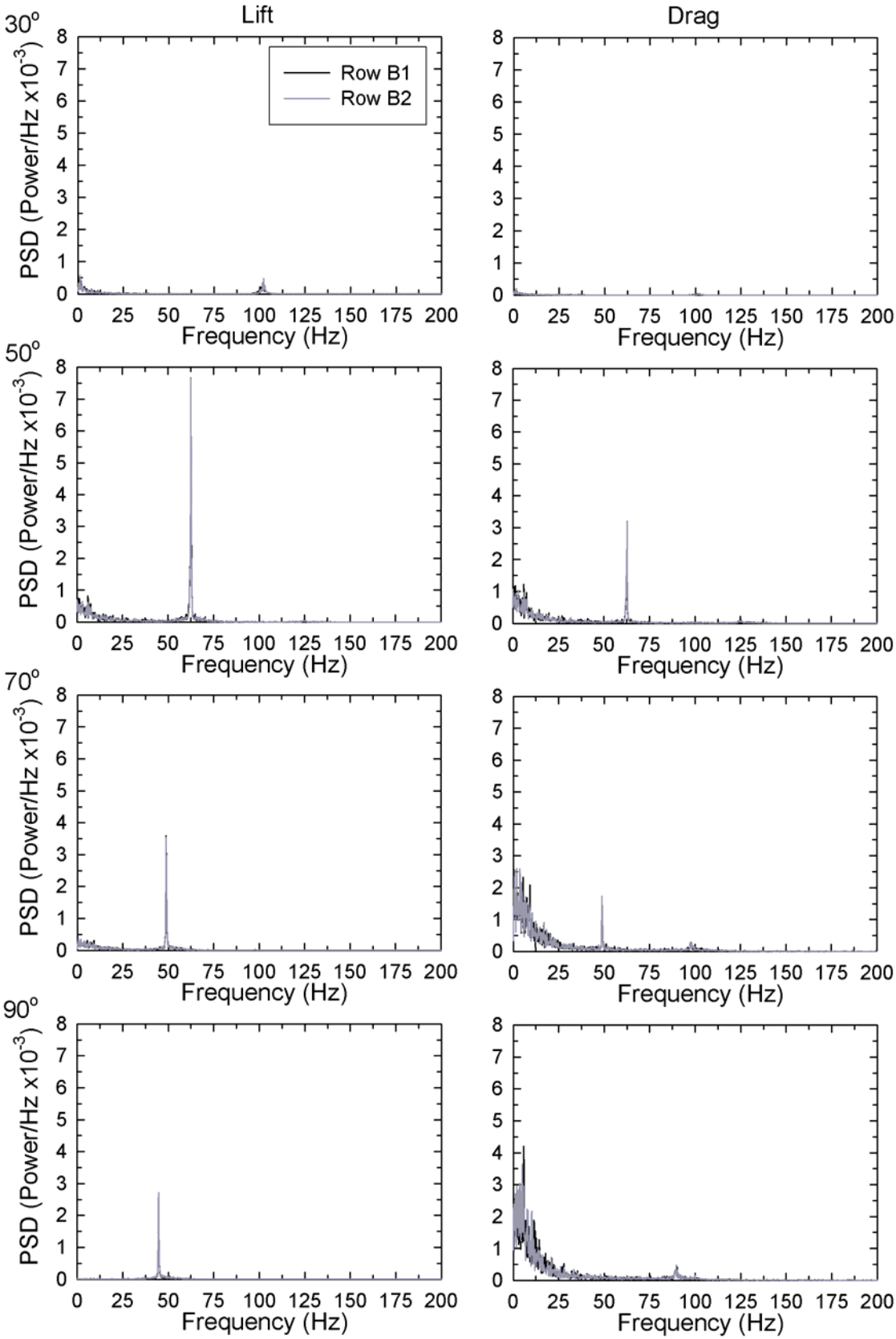

Figure 4 – Power Spectral Density (PSD) of lift and drag at various angles of attack (α).

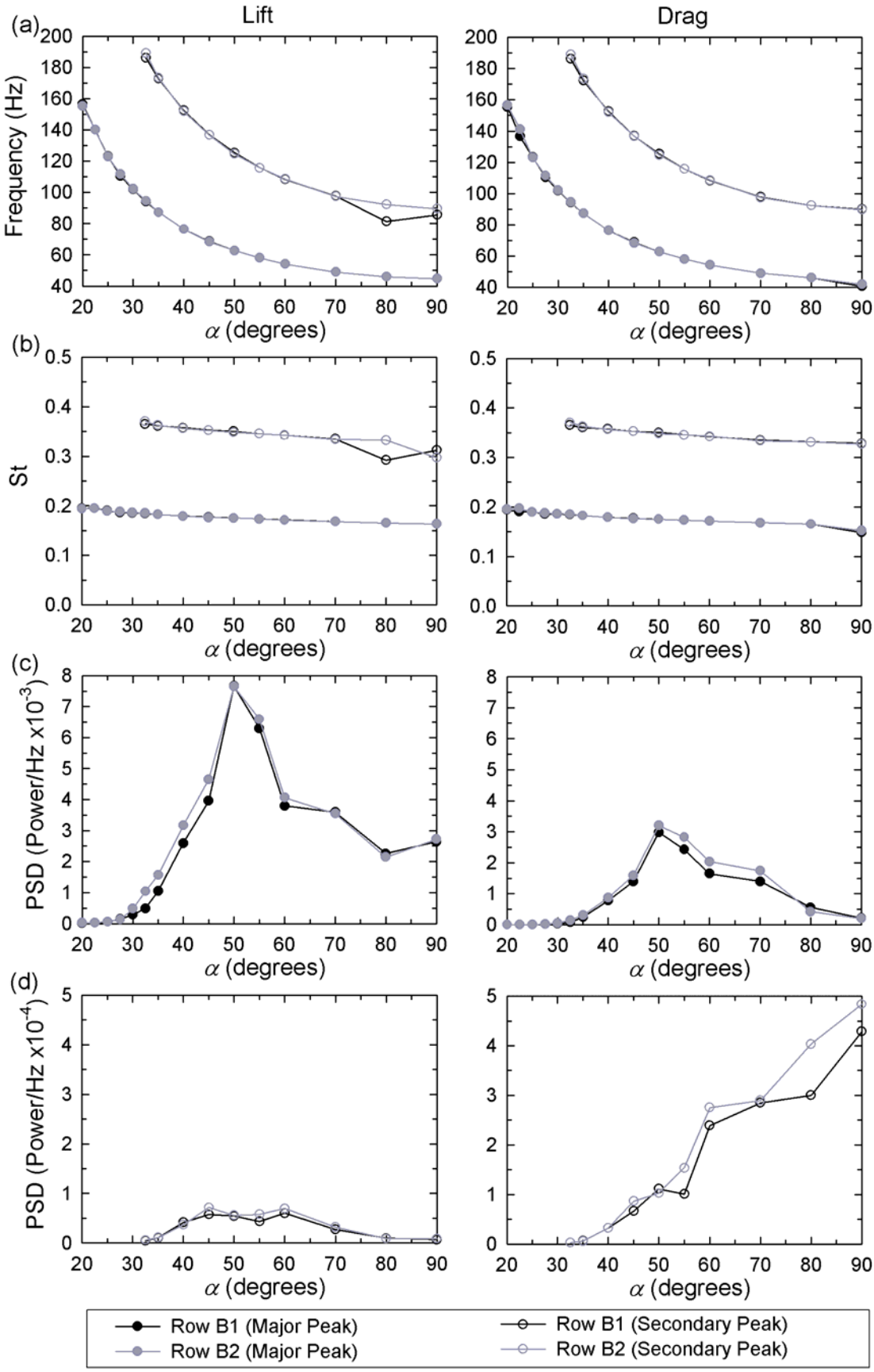

Figure 5 – (a) Frequency of the main (closed circles) and secondary (open circles) peaks, (b) this frequency expressed a Strouhal number (*St*), (c) the size of the main peak and (d) secondary peak all versus the angle of attack (α).

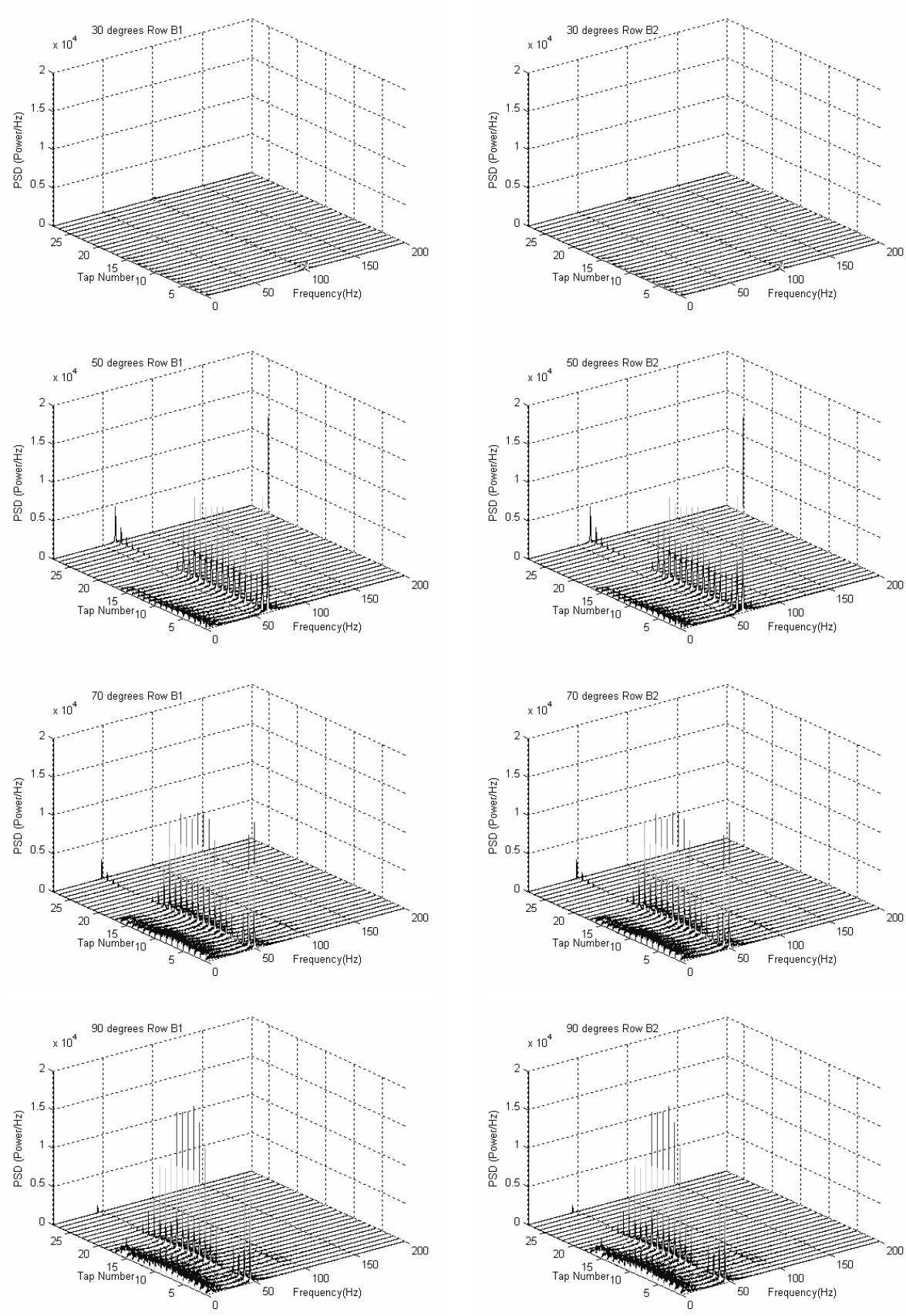

Figure 6 – Power Spectral Density (PSD) for each tap in Row B1 and Row B2 for angles of attack of 30, 50, 70 and 90 degrees. Tap numbering goes from 1 on the trailing edge across top surface to 15 at the leading edge and along the bottom surface to tap 28.

Figure 6 shows that the frequencies seen by taps in Row B1 and B2 are very similar. At α = 30° the main shedding peak is seen in the top surface taps (taps 1 to 15) and to a lesser extent in the bottom surface taps close to the trailing edge (around tap 28). This is similar for all cases. However these frequencies are more evident in either the drag or the lift depending on the α. The secondary frequency is more interesting. It is visible near the top trailing edge at α = 50 but the main vortex sheet obviously dominates what the tap sees. However it moves to mid chord by α = 90° and provides the major shedding peak observed by these taps. This would seem to indicate the location of interaction of the vortex sheets as the lower frequency, the influence of one sheet, is not evident.

The other interesting feature is the low frequency information concentrated in taps on the surface nearest the wake (the top surface of the airfoil). This is possibly related to slow fluctuations in the over all wake, but unfortunately there is not enough information in the surface pressure measurements to determine its exact cause. Similar low frequencies were found by Nakamura[8] in his investigation of bluff bodies with after bodies.

CONCLUSIONS

At high α distinct shedding frequencies were found in both the lift and the drag forces. A secondary frequency was found at a half of the main frequency, as would be expected for a symmetric bluff body. The asymmetry in the flow resulting from an airfoil at non-zero α caused both frequencies to be present in both the lift and drag. These frequencies were able to be scaled by the width of the chord normal to the freestream into a *St* that was almost independent of α. The major shedding peak occurred at α=50° in the lift.

ACKNOWLEDGEMENTS

Primary support for this research program was provided by a Monash Graduate Scholarship. SP Systems, Australia kindly donated the carbon fibre and epoxy used to construct the airfoil section. Finally thanks must go to the Mechanical Engineering workshop staff, especially Mr. Don McMaster and Mr. John Hick, for their advice and the construction of the airfoil section and supports.

REFERENCES

1. Hansen, A.C., and C.P. Butterfield, "Aerodynamics of Horizontal-Axis Wind Turbines," *Annual Review of Fluid Mechanics*, Vol. 25 No. 1993, pp. 115-49.
2. Hansen, M.H., "Improved Modal Dynamics of Wind Turbines to Avoid Stall-induced Vibrations," *Wind Energy*, Vol. 6 No. 2003, pp. 179-95.
3. Fage, A., and F.C. Johansen, "The Structure of Vortex Sheets," *Phil. Mag. S.*, Vol. 7 No. 28, 1928, pp. 417-41.
4. Roshko, A., "On the wake and drag of bluff bodies," *Journal of the Aeronautical Sciences*, Vol. No. 1955, pp. 124-32.
5. Chen, J.M., and Y.-C. Fang, "Strouhal numbers of inclined flat plates," *Journal of Wind Engineering and Industrial Aerodynamics*, Vol. 61 No. 1996, pp. 99-112.
6. Szepessy, S., and P.W. Bearman, "Aspect Ratio and End Plate Effects on Vortex Shedding from a Circular Cylinder," *Journal of Fluid Mechanics*, Vol. 234 No. 1992, pp. 191-217.
7. Irwin, H.P.A.H., K.R. Cooper, and R. Girard, "Correction of distortion effects caused by tubing systems in measurements of fluctuating pressures," *Journal of Wind Engineering and Industrial Aerodynamics*, Vol. 5 No. 1979, pp. 93-107.
8. Nakamura, Y., "Vortex Shedding from Bluff Bodies and a Universal Strouhal Number," *Journal of Fluids and Structures*, Vol. 10 No. 1996, pp. 159-71.